Axonal targeting of Caspr2 in hippocampal neurons via selective somatodendritic endocytosis

Christophe Bel[1], Ksénia Oguievetskaia[2], Christophe Pitaval[1], Laurence Goutebroze[2] and Catherine Faivre-Sarrailh[1,*]

[1]Centre de Recherche en Neurobiologie et Neurophysiologie de Marseille, UMR 6231 CNRS, Université de la Méditerranée Aix-Marseille II, Marseille 13916, France
[2]Unité Mixte de Recherche-S 839, Inserm, Université Pierre et Marie Curie, Institut du Fer à Moulin, Paris 75005, France
*Author for correspondence (catherine.sarrailh@univmed.fr)

Accepted 13 July 2009
Journal of Cell Science 122, 3403-3413 Published by The Company of Biologists 2009
doi:10.1242/jcs.050526

Summary

Contactin-associated protein 2 (Caspr2) is a neuronal membrane protein that is mutated in autism and related disorders. Although it is highly enriched at juxtaparanodes of Ranvier where it is essential for Shaker-type K^+ channel clustering, little is known about its function and regulation. In the present study, we examined the polarized expression of Caspr2 in hippocampal neurons using extracellular hemagglutinin (HA)-tagged Caspr2 constructs. We found that Caspr2 was targeted to the axonal surface, but colocalized with early endosomes in the somatodendritic compartment. The inhibition of endocytosis using a Dynamin-1 mutant or treatment with Dynasore prevented Caspr2 internalization from the dendrites and cell body. We identified a short sequence included into the 4.1B-binding domain that is required for the endocytosis of Caspr2. This sequence contains a protein kinase C (PKC) substrate motif on Thr1292, and point mutation of this residue or treatment with a PKC inhibitor prevented the somatodendritic internalization of Caspr2. Thus, the PKC-dependent trafficking of Caspr2 underlies its polarized expression in hippocampal neurons.

Supplementary material available online at
http://jcs.biologists.org/cgi/content/full/122/18/3403/DC1

Key words: Node of Ranvier, Juxtaparanode, Neuronal polarity, PKC phosphorylation

Introduction

Neurons are highly polarized cells, and the establishment of their cellular subdomains such as the synapses or nodes of Ranvier requires polarized sorting into axonal and somatodendritic compartments and the targeting of membrane proteins to specific locations. Several distinct mechanisms have been reported for the axonal sorting of membrane proteins, including selective axonal targeting along the secretory or endosomal pathways and uniform delivery and selective elimination from the dendritic plasma membrane (Horton and Ehlers, 2003; Wisco et al., 2003; Heusser and Schwappach, 2005; Arnold, 2007). Ion channels are spatially segregated into subdomains in myelinated axons and this organization is essential for generating fast saltatory conduction (Waxman and Ritchie, 1993). Voltage-gated sodium channels are concentrated at the node of Ranvier and Shaker-type Kv1 potassium channels are segregated at juxtaparanodes. The paranodal junctions that anchor the terminal myelin loops to the axon act as a fence separating these two regions (Peles and Salzer, 2000; Brophy, 2001; Girault and Peles, 2002). Ion channels are associated with complexes of cell adhesion molecules (CAMs), which mediate contacts between axon and glial cells and influence the lateral segregation of membrane domains along axons (Eshed et al., 2005; Schafer and Rasband, 2006). It is yet unknown whether preformed complexes of CAMs and channels are addressed to the axonal membrane or whether multiple intrinsic signals are acting to induce polarized sorting of these membrane molecules.

Contactin-associated protein 2 (Caspr2) is a cell adhesion molecule of the neurexin superfamily, which is implicated in the clustering of the Kv1 potassium channels at juxtaparanodes (Poliak et al., 1999). The extracellular domain of Caspr2 mediates interaction with transient axonal glycoprotein 1 (TAG-1), an Ig-CAM expressed by both the axonal and the opposing glial membranes (Traka et al., 2002). In Caspr2- and TAG-1-deficient mice, the positioning of potassium channels at juxtaparanodes is altered (Poliak et al., 2003; Traka et al., 2003). The Caspr2 cytoplasmic tail contains a juxtamembrane conserved region for the binding of the cytoskeleton adaptor 4.1B (Denisenko-Nehrbass et al., 2003), a protein with a 4.1, ezrin, radixin, moesin (FERM) domain and a C-terminal PSD-95/Discs large/Zonula-occludens-1 (PDZ)-binding sequence. Kv1 molecules also contain a C-terminal PDZ-binding sequence and associate with the scaffolding molecules post-synaptic density protein (PSD)-95 (Rasband et al., 2002) and PSD-93 (Ogawa et al., 2008). The exact mechanisms implicated in the coclustering of Caspr2 and Kv1 channels and their recruitment at juxtaparanodes are still unknown. However, the intracellular cues implicated in neuronal polarization of Kv1 channels have been determined using cultured hippocampal neurons. Kv1.2 is selectively sorted in axonally transported vesicles through the interaction of its β-subunits with the kinesin KIF3 (Gu et al., 2006). By contrast, nothing is known about the axonal targeting of Caspr2.

Recent independent studies have implicated mutations in the Caspr2 locus (*CNTNAP2*) in type-1 autism or related diseases with language impairment (Burbach and Van der Zwaag, 2009; Stephan, 2008). Alterations in the Caspr2 protein in these neuropsychiatric disorders may correspond to loss-of-function mutations such as protein truncation. It is therefore crucial to increase our knowledge about the trafficking and regulated cell surface expression of Caspr2 in the central nervous system.

Here, we examined the molecular basis for the axonal localization of Caspr2 in hippocampal neurons. We show that Caspr2 is delivered to both the somatodendritic and axonal compartments and its polarized expression is achieved through the selective endocytosis from the somatodendritic plasma membrane. A short sequence included in the 4.1B-binding domain of Caspr2 is implicated in the selective depletion from the somatodendritic plasma membrane. We conclude that distinct mechanisms are implicated for the axonal restriction of the two juxtaparanodal proteins Kv1.2 and Caspr2.

Results

Caspr2 is selectively expressed at the axonal membrane of hippocampal neurons during maturation

First, we examined the expression of endogenous Caspr2 in rat hippocampal neurons in culture. Immunofluorescence staining for Caspr2 was performed on permeabilized cells using an antibody directed against the cytoplasmic region, which did not allow the specific detection of the protein pool expressed at the cell surface. Caspr2 was slightly expressed in neurons after 8 days in vitro (DIV8). Caspr2 immunoreactivity was detected in the soma and axon, but not in dendrites, and was observed at the axonal initial segment as shown using double staining for Ankyrin-G (supplementary material Fig. S1) and as previously reported (Ogawa et al., 2008).

To analyze more specifically the distribution of Caspr2 at the neuronal cell surface, we expressed in hippocampal neurons a Caspr2 construct with an extracellular hemagglutinin (HA) epitope inserted downstream of the signal peptide (Caspr2-HA) (Fig. 1A). Live neurons were immunostained with anti-HA mAb and HA-tagged Caspr2 was selectively detected at the axonal surface in hippocampal neurons at DIV8 (Fig. 1B). As shown using double staining for the somatodendritic marker microtubule-associated protein 2 (MAP2), Caspr2 was faintly expressed at the surface of the dendritic compartment similarly to the endogenous molecule (Fig. 1B). Quantitative analysis was performed to evaluate the ratio between axonal (A) and somatodendritic (SD) surface labeling (A/SD ratio >3) and confirmed the visual observations (Fig. 1J).

The highly restricted axonal distribution of Caspr2 was observed in transfected neurons until DIV22, which was the latest developmental stage examined (supplementary material Fig. S2). Conversely, before DIV7, Caspr2 expression was nonpolarized because it was strongly expressed at the axonal and somatodendritic surface from DIV2 to DIV6, indicating that the polarized expression of Caspr2 is regulated during neuronal maturation (supplementary material Fig. S2).

Caspr2 undergoes internalization in the somatodendritic compartment of hippocampal neurons

To characterize the distribution of the intracellular pool of Caspr2, we performed fixation and permeabilization of hippocampal neurons transfected with HA-Caspr2 at DIV8. Caspr2 was detected in many vesicles in the somatodendritic compartment and it colocalized with EEA1, a marker of early endosomes (Fig. 1C). Quantitative analysis indicated that 43% of the early endosomes were positive for both Caspr2 and EEA1 (Fig. 1K), suggesting that Caspr2 could undergo internalization via endocytosis in neurons. Caspr2 was also detected in vesicular structures that were negative for EEA1, indicating that it might be processed along the recycling or lysosomal pathways.

We attempted to determine whether there was a region of Caspr2 that contained a signal for endocytosis. We first generated a construct deleted from the cytoplasmic region of the protein by inserting a stop codon at the end of the transmembrane sequence (Caspr2Δcyt) (Fig. 1A). This deletion mutant was uniformly detected at the cell surface of hippocampal neurons at DIV8. As shown in Fig. 1D, the axon and also the somatodendritic compartment were strongly labeled for Caspr2Δcyt after live immunostaining using anti-HA antibody. Very few vesicles were double stained for EEA1 and HA (6%) in the somatodendritic compartment of neurons, indicating that Caspr2Δcyt was faintly internalized (Fig. 1E,K). These observations demonstrate that the cytoplasmic region of Caspr2 is required for selective axonal distribution of the protein and strongly suggested that endocytosis might regulate its somatodendritic localization.

Reciprocally, we tested whether the extracellular region has a role in the polarized targeting of Caspr2. We generated a construct with the transmembrane and cytoplasmic regions of Caspr2 fused with the HA epitope and GFP downstream of the NrCAM signal peptide (GFP-Caspr2cyt) (Fig. 1A). The control construct contained the transmembrane and cytoplasmic region of NrCAM fused with the HA epitope and GFP downstream of the NrCAM signal peptide (GFP-NrCAMcyt). It displayed a nonpolarized distribution at the cell surface of hippocampal neurons (Fig. 1F) and did not colocalize with early endosomes (Fig. 1G). By contrast, and as observed for the full-length Caspr2, GFP-Caspr2cyt was selectively expressed at the axonal surface (A/SD ratio = 2) (Fig. 1H,J) and internalized in the somatodendritic compartment, in which 56% of the early endosomes were positive for HA (Fig. 1I,K). Thus, the cytoplasmic region of Caspr2 contains a sufficient signal for the polarized targeting and somatodendritic endocytosis of the molecule.

The cytoplasmic region of Caspr2 contains a signal for endocytosis in COS-7 cells

To further evaluate whether the cytoplasmic region of Caspr2 contains a signal mediating endocytosis, immunoendocytosis assays were performed on transfected COS-7 cells. Cells expressing the HA-tagged constructs, Caspr2, GFP-NrCAMcyt and GFP-Caspr2cyt were first exposed to the anti-HA mAb at 4°C and internalization was allowed for 30 minutes by incubating cells at 37°C. The control construct GFP-NrCAMcyt was only detected at the cell surface and did not colocalize with EEA1-positive endosomes after the 30 minute internalization period (supplementary material Fig. S3A,B,B′). Caspr2 and GFP-Caspr2cyt were detected at the cell surface of COS-7 cells under control conditions (time = 0 minutes) (supplementary material Fig. S3C,E) but colocalized with EEA1-positive endosomes after incubation at 37°C (supplementary material Fig. S3D,D′,F,F′). Thus, the cytoplasmic region of Caspr2 contains a signal for endocytosis in both neuronal and non-neuronal cells.

The polarized expression of Caspr2 is achieved through endocytic elimination from the somatodendritic surface

To determine whether Caspr2 is preferentially internalized in the somatodendritic compartment, immunoendocytosis assays were performed on transfected neurons. Neurons at DIV8 were incubated with anti-HA mAb for 1 hour at 37°C to allow endocytosis, and then the surface and internalized pools of Caspr2 were sequentially labeled before and after permeabilization using two different fluorescently tagged secondary antibodies. As shown in Fig. 2A, the internalized pool of Caspr2 (red) can be distinguished from surface labeling (green). Numerous endocytic Caspr2-containing vesicles (red and not green) were present in the soma and proximal

dendrites (36±3.8 vesicles per neuron), whereas very few labeled vesicles were detected in the proximal axon (1.2±0.2 vesicles per neuron) (Fig. 2A,B) or at the growth cone (1±0.4 vesicles per neuron) (supplementary material Fig. S4A). Since axons and dendrites were not easily visualized along their entire length, we estimated the ratio of vesicles per neurite length was seven times greater in dendrites than it was in axons (Fig. 2B). We also examine whether Caspr2 was co-internalized with transferrin in the somatodendritic compartment. Immunoendocytosis assays were performed on transfected neurons incubated with Alexa-Fluor-594-

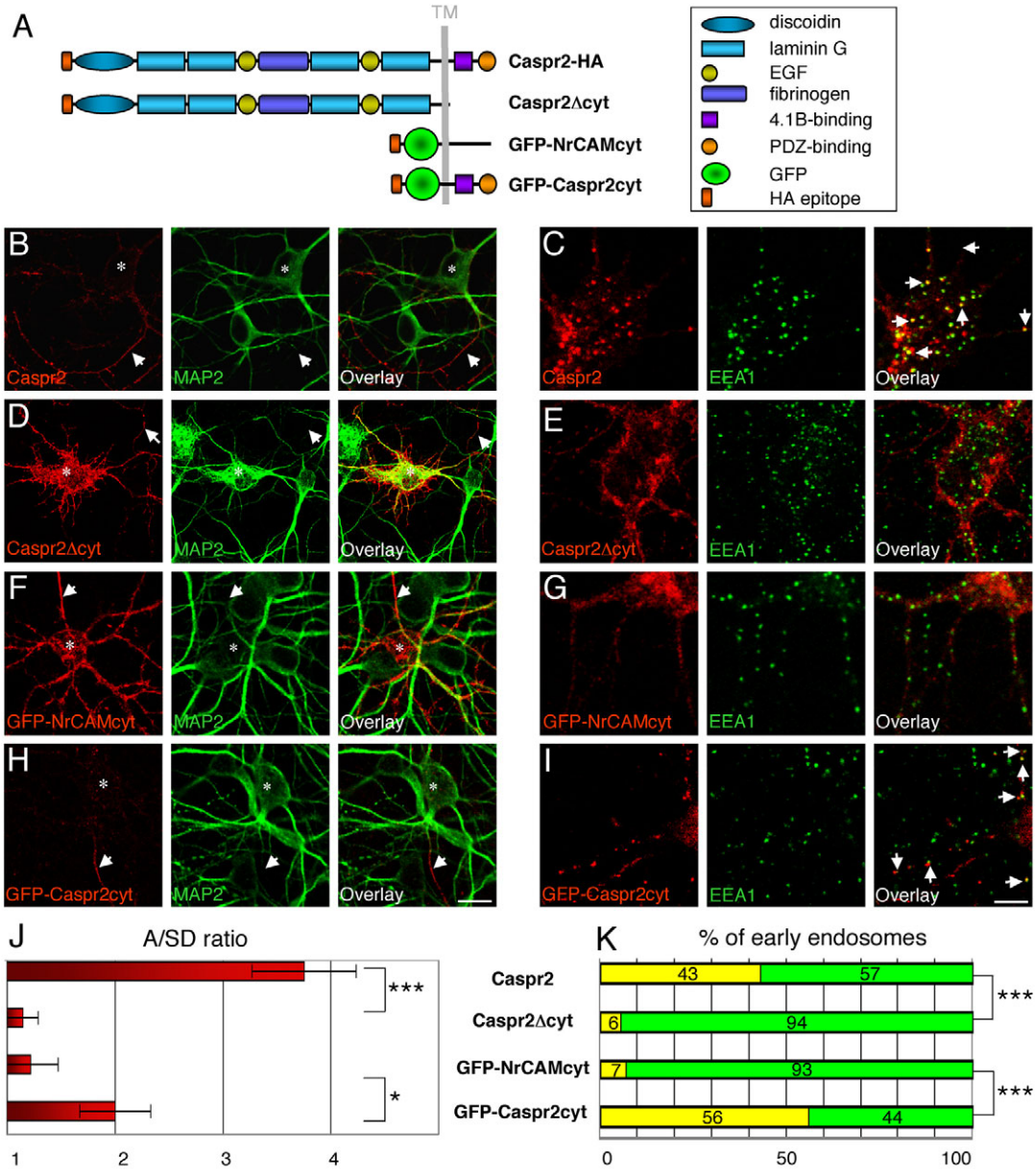

Fig. 1. The cytoplasmic tail of Caspr2 contains a signal for axonal targeting and somatodendritic internalization. (A) Schematic representation of Caspr2 mutant constructs. The Caspr2 extracellular region contains a discoidin domain, four laminin G and two EGF-like domains and a fibrinogen domain. The Caspr2 cytoplasmic region contains a 4.1B-binding domain and a C-terminal PDZ-binding sequence. A HA epitope was inserted downstream of the signal peptide in Caspr2-HA. The control construct GFP-NrCAMcyt contains the NrCAM signal peptide, the HA epitope, GFP and the transmembrane and cytoplasmic regions of NrCAM. The GFP-Caspr2cyt contains the NrCAM signal peptide, the HA epitope, GFP and the transmembrane and cytoplasmic regions of Caspr2. (B-I) DIV8 hippocampal neurons transfected with Caspr2 (B,C), Caspr2Δcyt (D,E), GFP-NrCAMcyt (F,G) or GFP-Caspr2cyt (H,I). (B,D,F,H) Neurons were surface-labeled for the extracellular epitope HA (red), and stained for the somatodendritic marker MAP2 (green, pseudocolor in F and H). Soma of transfected neurons are indicated with asterisks and axons with white arrows. (J) Fluorescence intensities of axonal and somatodendritic surface labeling for HA were measured and the ratio calculated (A/SD ratio). Values are means ± s.e.m. Caspr2 and GFP-Caspr2cyt are targeted to the axonal surface whereas Caspr2Δcyt and GFP-NrCAMcyt display uniform axonal and somatodendritic surface labeling. (C,E,G,I) Fixed and permeabilized cells were double-stained for HA (red) and EEA1 (green, pseudocolor in G and I). Double-stained early endosomes are indicated with white arrows. (K) The percentage of early endosomes positive for EEA1 only (green) or double-labeled for the transfected protein (yellow) was measured. Caspr2 and GFP-Caspr2cyt colocalized with the early endosomes marker EEA1 within the somatodendritic compartment, whereas Caspr2Δcyt and GFP-NrCAMcyt did not. ANOVA indicates a significant difference between means. *P<0.05; ***P<0.001. Scale bars: 15 µm (B,D,F,H) and 7 µm (C,E,G,I).

conjugated-transferrin. As shown in supplementary material Fig. S4B,C, numerous vesicles were double-stained for Caspr2 and transferrin. Quantitative analysis indicated that 54±6.6% (n=15) of the Caspr2-positive endocytic vesicles contained transferrin.

Next, to evaluate whether the somatodendritic endocytosis of Caspr2 influences its polarized expression, endocytosis was prevented in transfected hippocampal neurons using two different assays. First, neurons were cotransfected with wild-type Dynamin-

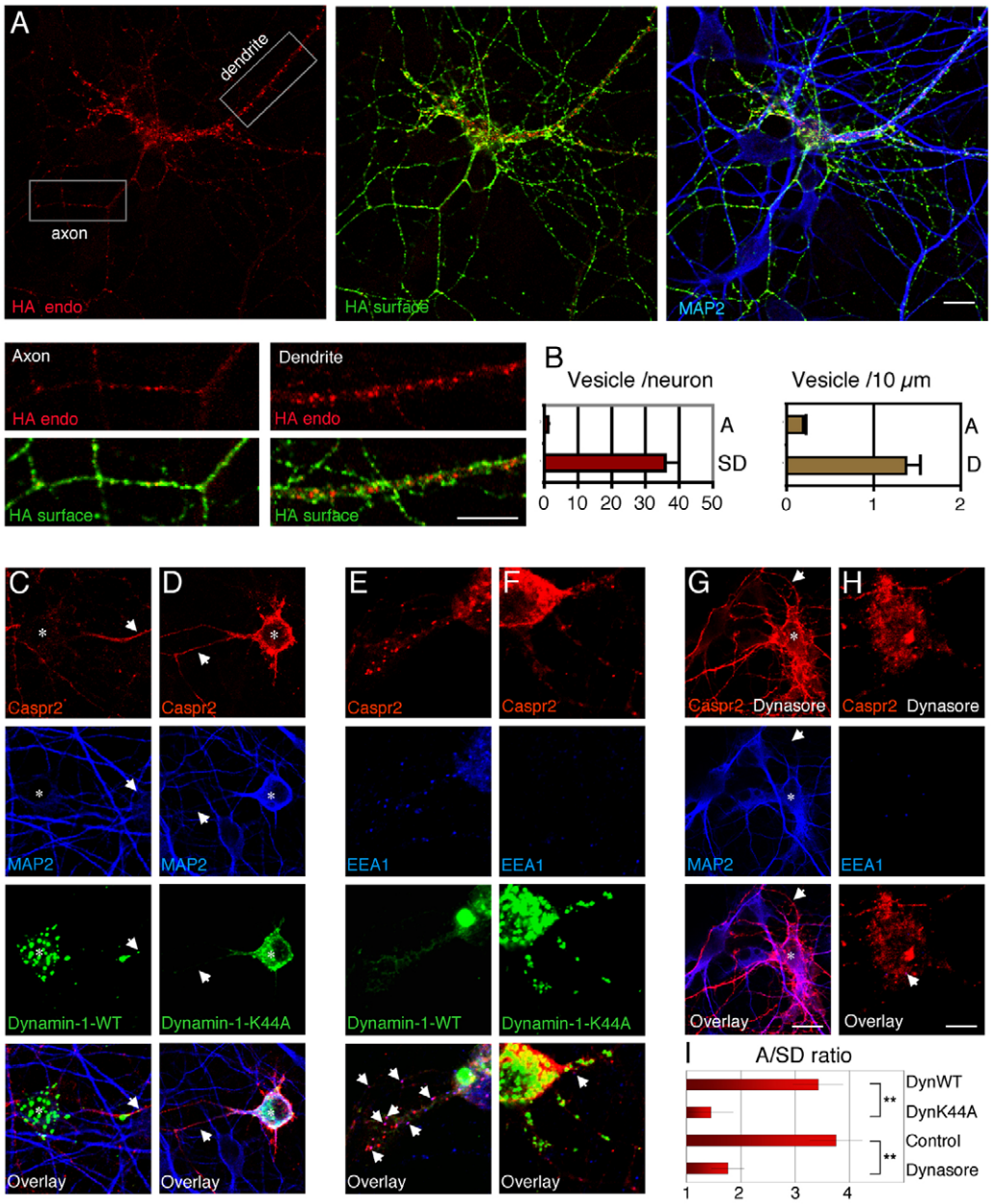

Fig. 2. Dynamin-dependent endocytosis underlies the removal of Caspr2 from the somatodendritic surface. (A) DIV8 hippocampal neuron transfected with Caspr2. Internalization of Caspr2 was mediated using anti-HA mAb for 1 hour at 37°C. Surface labeling (HA surface, green) was performed using Alexa Fluor 488 anti-rat immunoglobulins at 18°C. Neurons were fixed, permeabilized and the internalized pool of HA-tagged Caspr2 was stained (HA endo, red) using Alexa Fluor 568 anti-rat immunoglobulins. Neurons were stained for MAP2 (blue). The lower panels are enlargements of the boxed areas of upper panels, showing internalization of Caspr2 in axonal and dendritic compartments. (B) Quantification of the number of Caspr2-internalized vesicles (red and not green) per neuron in axonal (A) and somato-dendritic (SD) compartments is shown on the left. Graph on the right shows the ratio of vesicles per neurite length in axons (A) and dendrites (D) for 10 neurons. (C-F) DIV8 hippocampal neurons cotransfected with Caspr2 and wild-type Dynamin-1 (Dynamin-1-WT) (C,E), or mutant Dynamin-1-K44A (D,F). (G,H) DIV8 hippocampal neurons transfected with Caspr2, treated with Dynasore 30 hours after transfection, and immunostained 18 hours after treatment. Neurons were surface-labeled for HA (red) and stained for MAP2 (blue) (C,D,G) or permeabilized and double-stained for HA (red) and EEA1 (blue) (E,F,H). The fluorescence of GFP-tagged Dynamin-1 was detected directly (green). White arrows indicate axons and asterisks indicate the soma of transfected neurons in C,D,G and early endosomes double-labeled for HA-tagged Caspr2 in E,F,H. (I) A/SD ratio; means ± s.e.m. (ANOVA, $^{**}P<0.01$). Cotransfection of Dynamin-1-WT with Caspr2 did not modify the polarized expression of Caspr2 nor its somatodendritic endocytosis (C,E), whereas in the presence of Dynamin-1-K44A or after treatment with Dynasore, Caspr2 was highly expressed at the somatodendritic surface (D,G) and the number of EEA1-positive vesicles was dramatically reduced (F,H). Scale bars: 10 μm (A), 15 μm (C,D,G) and 7 μm (E,F,H)

1 or a mutant form of Dynamin-1 (Dynamin-1-K44A), which is defective in GTP binding and blocks the Dynamin-dependent endocytosis (Damke et al., 1994). Caspr2 localization was normally restricted to the axonal surface and internalized in somatodendritic endosomes in neurons cotransfected with the wild-type Dynamin-1 fused with GFP at DIV8 (Fig. 2C,E,I). By contrast, cotransfection with Dynamin-1-K44A prevented the formation of early endosomes as evaluated using anti-EEA1 immunostaining (Fig. 2F), and Caspr2 was strongly expressed at the somatodendritic surface and exhibited a nonpolarized distribution (Fig. 2D,I).

Neurons were also treated with Dynasore, a cell-permeable inhibitor of Dynamin that blocks coated vesicle formation (Macia et al., 2006). Thirty hours after transfection, cells were incubated with Dynasore for a period of 18 hours. The endocytic pathways were strongly inhibited, as indicated by the loss of immunostaining for EEA1 (Fig. 2H), and Caspr2 was strongly expressed at the cell surface of both the somatodendritic and axonal compartments (Fig. 2G,I). Altogether, our data indicate that endocytosis of Caspr2 in the somatodendritic compartment is required for its polarized expression in hippocampal neurons.

Caspr2 vesicular transport and insertion in the plasma membrane of hippocampal neurons

To analyze whether Caspr2 could be preferentially transported within axons, videomicroscopy experiments were performed using Caspr2 fused with GFP. Since Caspr2 contains a PDZ-binding site at its C-terminus, GFP was inserted at the N-terminus of the extracellular domain, downstream of the signal peptide (Fig. 3). Videomicroscopy analyses indicated that Caspr2-GFP was targeted to axons via anterograde axonal transport (Fig. 3A; supplementary material Movie 1). In axons, Caspr2-GFP was transported in vesicles of round or ovoid shape moving with a mean velocity of 1.05±0.11 μm/second from the cell bodies towards the growth cone (supplementary material Movie 2). In the cell bodies and large proximal dendrites, Caspr2-GFP was detected within numerous vesicles that exhibited fast and unoriented displacements that probably corresponded to endocytic vesicles (supplementary material Movie 3). In addition, anterograde transport of Caspr2-GFP was observed in distal dendrites (Fig. 3B; supplementary material Movie 4), with a mean velocity of 0.68±0.08 μm/second, which might correspond to secretory or endosomal vesicles. Caspr2 was transported preferentially in the anterograde direction, both in axons and dendrites (Fig. 3D), and thus did not exhibit polarized vesicular trafficking.

Next, we examined whether newly synthesized Caspr2 was inserted in the somatodendritic and/or axonal compartments after Brefeldin A block of exocytosis (Fache et al., 2004). Neurons at DIV7 were transfected with Caspr2, treated overnight with Brefeldin A and then, the surface expression of Caspr2 was analyzed at different time points after recovery. Intracellular accumulation of Caspr2 was observed immediately upon Brefeldin A removal (Fig. 3E), whereas no surface labeling was detected. After 1 hour of recovery, few cells exhibited surface labeling for Caspr2 and all the cells examined (n=30) were uniformly labeled in the somatodendritic and axonal compartments (Fig. 3F). After 2 hours of recovery, Caspr2 was enriched at the axonal membrane in 20% of transfected neurons (Fig. 3G), and was equally expressed at the surface of the somatodendritic and axonal compartments in most cells (n=63). These data suggest that neosynthesized Caspr2 is uniformly addressed to the axonal and somatodendritic plasma membrane.

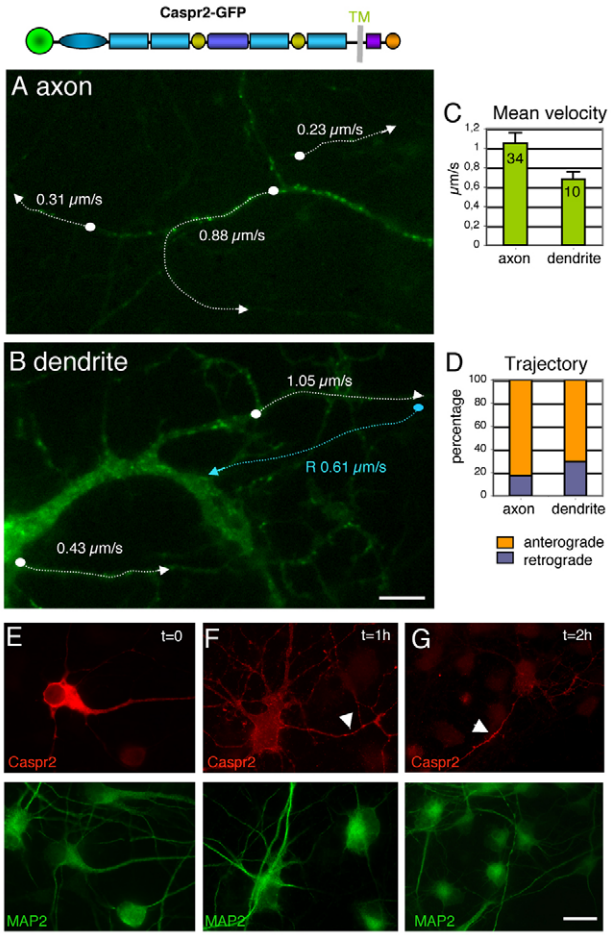

Fig. 3. Vesicular transport and insertion of Caspr2 at the plasma membrane in hippocampal neurons. Caspr2-GFP construct (top): GFP was inserted at the N-terminus of Caspr2 downstream of the signal peptide. Neurons were transfected at DIV9 with Caspr2-GFP and live imaging recorded at DIV10. Frames were collected at the rate of 1 per second for 120 seconds and the trajectories of Caspr2-GFP vesicles analyzed using the Metamorph tracking software. Representative frames in axons (A) or dendrites (B) corresponding to supplementary material Movies 1 and 4, respectively. Examples of anterograde (white) or retrograde (R, blue) vesicle tracking, with the mean velocity indicated. (C) Mean velocity of Caspr2-GFP vesicles, the number of tracked vesicles is indicated. (D) Percentage of anterograde and retrograde moving vesicles in axons and distal dendrites. (E-G) Cell-surface distribution of Caspr2 after Brefeldin A removal. DIV7 neurons were transfected with Caspr2 and treated 4 hours after transfection with 0.75 μg/ml Brefeldin A for 16 hours. (E) Upon Brefeldin A removal, neurons were fixed, permeabilized and double-stained for HA (red) and MAP2 (green). After 1 hour (F) and 2 hours (G) of Brefeldin A recovery, neurons were surface-labeled for HA (red) and double-stained for MAP2 (green). White arrows indicate axons. Note the uniform surface staining for Caspr2 of the axonal and somatodendritic compartments after 1 hour of recovery (F). 20% of cells exhibit a polarized expression of Caspr2 after 2 hours of recovery (G). Scale bars: 10 μm (A,B) and 15 μm (E-G).

The C-terminal region is not implicated in the polarized expression of Caspr2

To identify a cytosolic determinant implicated in the axonal targeting of Caspr2, deletion and mutant constructs were generated (supplementary material Fig. S5A). The cytoplasmic tail of Caspr2 contains a C-terminal consensus type II motif for the binding of PDZ proteins (EWLI). Association with a PDZ scaffolding molecule might be involved in the stabilization of Caspr2 at the axolemma.

In addition, the two extreme C-terminal amino acids (LI) might form a dileucine motif that mediates endocytosis (Bonifacino and Traub, 2003). Mutation of the PDZ-binding domain (EWLI to AGLI) and dileucine motif (EWLI to EWAA) did not modify the expression of Caspr2 at the axonal surface (supplementary material Fig. S5B,D,H) or its internalization in the somatodendritic compartment (supplementary material Fig. S5C,E,I). In addition, deletion of the C-terminal region (residues 1306-1331, Caspr2ΔCter) had no significant effect (supplementary material Fig. S5F,G,H,I), which demonstrates that the consensus PDZ-binding motif of Caspr2 is not responsible for its selective expression at the axonal surface in hippocampal neurons.

A determinant for endocytosis and polarized expression of Caspr2 is contained in the 4.1-binding domain

Next, we used mutational analysis to determine whether the 4.1-binding motif contributes to the axonal localization of Caspr2. The juxtamembrane domain of Caspr2 is highly conserved among the members of the Caspr family and contains a 4.1-binding motif that was first characterized in glycophorin C (Marfatia et al., 1995). It is conserved in other proteins that bind to FERM domains and is referred to as a GNP motif (glycophorin C, neurexin IV, paranodin) (Denisenko-Nehrbass et al., 2003). A large deletion (residues 1284-1305) of the N-terminal part of the cytoplasmic tail including the 4.1-binding domain (Caspr2Δ4.1) was generated (Fig. 4A). This deletion was previously shown to inhibit the interaction of Caspr2 with 4.1B in GST pull-down experiments (Denisenko-Nehrbass et al., 2003) and in cotransfected HeLa cells (L.G., unpublished results). As observed with Caspr2Δcyt, the Caspr2Δ4.1 mutant was uniformly expressed at the cell surface of hippocampal neurons at DIV8 (Fig. 4B,L) and was poorly internalized in the somatodendritic compartment (Fig. 4C,M).

Since 4.1B is associated with Caspr2 at the juxtaparanodes of myelinated axons (Denisenko-Nehrbass et al., 2003), we asked whether it could be also colocalized with Caspr2 in axons of hippocampal neurons. Immunofluorescence staining indicated that 4.1B is uniformly distributed in hippocampal neurons (not shown). We examined whether the association with 4.1 molecules intervened in the polarized expression of Caspr2 and evaluated the effect of point mutations of two residues Y1293 and H1294 (Fig. 4A), which are critical for the binding of 4.1 molecules (L.G., unpublished results). The mutants Caspr2-Y1293F and Caspr2-H1294A displayed a polarized expression in hippocampal neurons (Fig. 4D,F,L) and colocalized with EEA1-labeled vesicles as efficiently as wild-type Caspr2 (Fig. 4E,G,M). This mutational analysis suggests that the binding of 4.1B to Caspr2 might not be required for its somatodendritic internalization and axonal targeting.

To identify more precisely a region of the 4.1-binding motif that could enable Caspr2 endocytosis, we generated two complementary partial deletions: Caspr2Δ1293-1305 and Caspr2Δ1284-1292 (Fig. 4A). Caspr2Δ1293-1305 was highly expressed at the axonal surface (Fig. 4H,L) and was internalized in the soma and dendrites as efficiently as full-length Caspr2 (Fig. 4I,M). By contrast, the Caspr2Δ1284-1292 mutant was uniformly distributed at the cell membrane of hippocampal neurons (Fig. 4J,L) and poorly internalized in the soma and dendrites (Fig. 4K,M). Thus, the juxtamembrane sequence RYMFRHKGT within the 4.1-binding domain, is a determinant required for somatodendritic internalization and polarized surface expression of Caspr2. By contrast, deletion of all the other amino acids of the cytoplasmic tail had no effect. This determinant does not contain any canonical signal such as dileucine or Yxxϕ motifs for adaptor proteins of the clathrin-dependent pathway (Bonifacino and Traub, 2003).

The somatodendritic internalization of Caspr2 is regulated by PKC phosphorylation

The endocytosis motif of Caspr2 includes the sequence KGT, which corresponds to a canonical phosphorylation site [R/K]x[pS/pT] for protein kinase C (PKC) at T1292 (Fig. 5A) (Pearson and Kemp, 1991; Ubersax and Ferrell, 2007). We tested whether a membrane-permeable inhibitor of PKC interfered with Caspr2 internalization. Hippocampal neurons transfected with Caspr2 were incubated for 18 hours with Calphostin C and H89, inhibitors of PKC and PKA, respectively. The somatodendritic surface expression of Caspr2 was strongly enhanced after treatment with the PKC inhibitor (Fig. 5B) compared with the control (Fig. 5D). By contrast, this effect was not observed when the cells were similarly treated with H89 (Fig. 5C). To assess whether this effect of Calphostin C was specific to Caspr2, a CD4 chimera fused with the C-terminus of the sodium channel Nav1.2 was used as a control (Garrido et al., 2001). More precisely, we used a truncated construct Δ1871 that contains the dileucine motif implicated in its somatodendritic internalization, but which does not include PKC phosphorylation sites (Garrido et al., 2001). This chimera was selectively expressed at the axonal surface both in control and Calphostin-C-treated neurons (Fig. 5E). Next, we examined the effect of Calphostin C on the somatodendritic internalization of Caspr2 using immunoendocytosis assays. The number of Caspr2 endocytic vesicles was strongly reduced in the soma of Calphostin-C-treated neurons, whereas transferrin uptake did not appear to be altered (Fig. 5F,G).

Because PKC can phosphorylate multiple targets, we wanted to determine whether the direct phosphorylation of Caspr2 by PKC was implicated in Caspr2 dendritic internalization. In vitro kinase assays were performed with GST fused to the cytoplasmic region of Caspr2. In the presence of PKC, Caspr2-GST was strongly phosphorylated as visualized by autoradiography (Fig. 5H). Since T1292 is the only putative phosphorylation site for PKC in the cytoplasmic region of Caspr2, we generated a Caspr2 construct with a mutation of this residue to alanine. This mutation prevented the depletion of Caspr2 from the somatodendritic surface (Fig. 6A,B). In accordance, internalization of the T1292A mutant (Fig. 6D) was strongly reduced compared with wild-type Caspr2 (Fig. 6C). Quantitative analysis of immunoendocytosis assays indicated that the mutation T1292A had a similar effect to the deletion of the cytoplasmic tail or endocytic motif 1284-1292 (Fig. 6E). Thus, our data strongly indicate that the endocytosis of Caspr2 governs its cell-surface presentation in a PKC-regulated manner.

Discussion

To obtain a better understanding of how neurons selectively target ion channels and CAMs to discrete subdomains of nerve, we analyzed the primary events at the basis of the polarized expression of Caspr2 in hippocampal neurons. We showed that Caspr2 is uniformly addressed to the plasma membrane of dendrites and axons, and is recognized by the endocytic pathway for clearance from the somatodendritic compartment. We identified a short determinant in the cytosolic juxtamembrane region that is essential for Caspr2 internalization. The polarized expression of Caspr2 into axons results from compartment-specific endocytosis as reported for the Nav1.2 sodium channels (Fache et al., 2004) and differs from the polarized vesicular trafficking of the Kv1.2 channels (Heusser and Schwappach, 2005).

The compartmentalization of the voltage-gated Nav1.2 sodium channels at the axonal initial segment and nodes of Ranvier has been proposed to rely on elimination-retention mechanisms (Fache et al., 2004). As a first step, the Nav1.2 channels would need to be uniformly delivered at the plasma membrane and subsequently eliminated from the somatodendritic compartment. Motifs from Nav1.2 that dictate endocytic elimination have been identified in the cytosolic C-terminal region and loop II-III. Restriction of Nav1.2 to the axonal initial segment would then be mediated by Ankyrin-G tethering via an Ankyrin-binding site in the loop II-III (Garrido et al., 2001; Garrido et al., 2003; Lemaillet et al., 2003). The endocytic motif located in the same loop would be required for the clearance of Nav1.2 from the distal part of the axon.

By contrast, the axonal targeting of the voltage-gated potassium channel Kv1.2 does not depend upon its internalization. Kv1.2 contains a signal for its direct delivery to axons through polarized vesicular trafficking. The axonal transport of Kv1.2 is mediated by its interaction with the KIF3 kinesin and requires the T1 tetramerization domain that is implicated in the binding of the channel β-subunits (Gu et al., 2003; Gu et al., 2006). The Kv1.2 T1 domain can act as a dominant signal for axonal targeting when fused to the normally non-polarized CD4 or normally dendritic

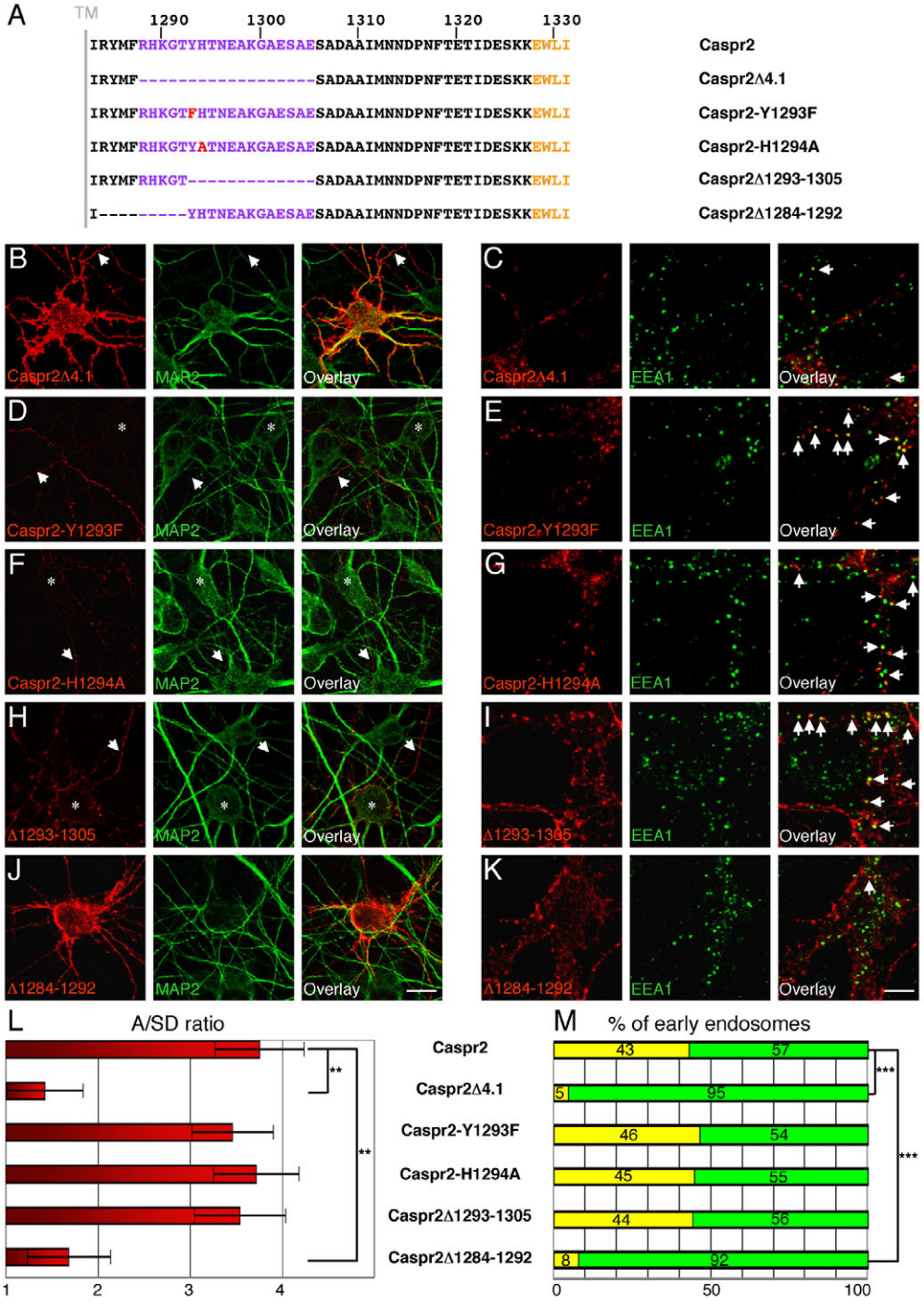

Fig. 4. The 4.1-binding domain contains a determinant implicated in the somatodendritic internalization of Caspr2. (A) Mutations and deletions in the 4.1-binding domain of Caspr2. The 4.1-binding domain is indicated in violet and the C-terminal PDZ-binding sequence in orange. (B-K) DIV8 hippocampal neurons transfected with Caspr2Δ4.1 (B,C), Caspr2-Y1293F (D,E), Caspr2-H1294A (F,G), Caspr2Δ1293-1305 (H,I) or Caspr2Δ1284-1292 (J,K). (B,D,F,H,J) Neurons were surface-labeled for HA (red), and stained for MAP2 (green). Soma of transfected neurons are indicated with asterisks and axons with white arrows. (L) A/SD ratios; means ± s.e.m. $^{**}P<0.01$, compared with control Caspr2 (ANOVA). (C,E,G,I,K) Cells permeabilized and double-stained for HA (red) and EEA1 (green). Double-stained early endosomes are indicated with white arrows. The percentage of early endosomes positive for EEA1 only (green) or double-labeled for the transfected protein (yellow) was determined (M). $^{***}P<0.001$ compared with control Caspr2 (ANOVA). Deletion of the 4.1-binding domain (B,C) or of the N-terminus of this domain (residues 1284-1292) (J,K) prevented the somatodendritic elimination of Caspr2. The point mutations Y1293F and H1294A had no effect (D,E,F,G). Deletion of residues 1293-1305 did not modify the axonal targeting (H) or somatodendritic endocytosis (I) of Caspr2. Scale bars: 15 μm (B,D,F,H,J) and 7 μm (C,E,G,I,K).

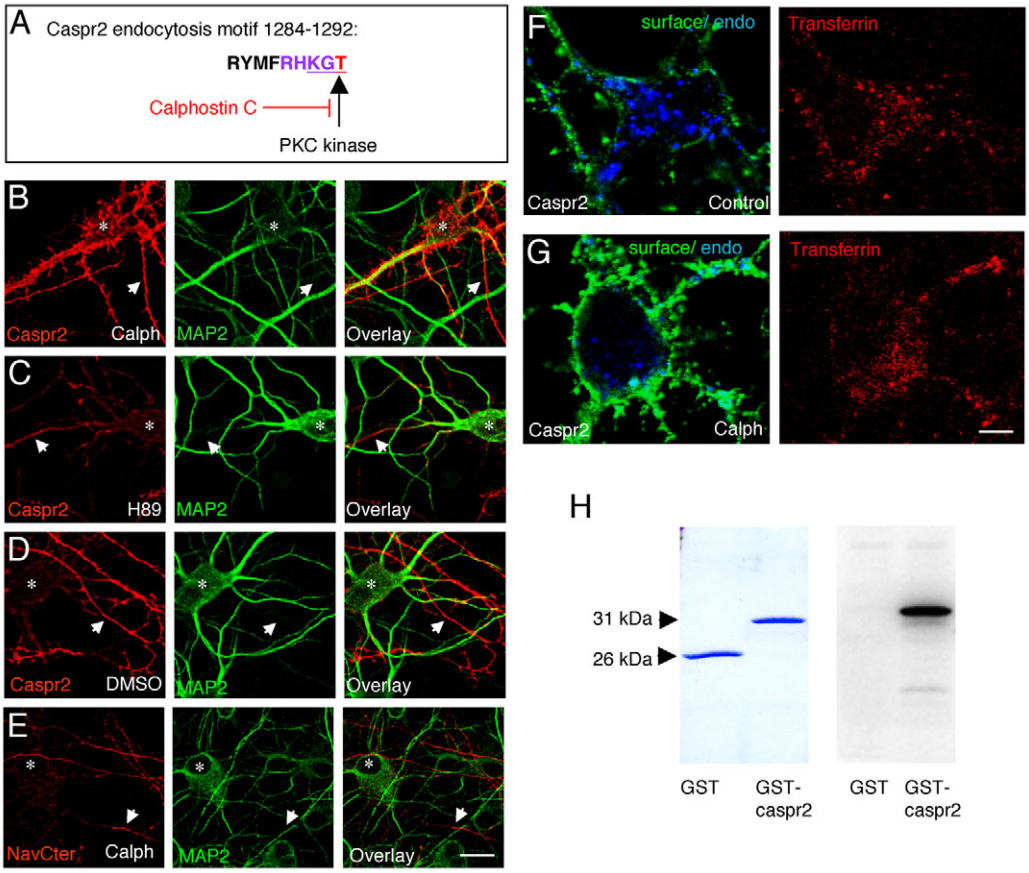

Fig. 5. The somatodendritic internalization of Caspr2 requires PKC phosphorylation. (A) The Caspr2 sequence implicated in endocytosis contains a putative substrate motif KGT for the phosphorylation of T1292 by PKC. Calphostin C is an inhibitor for PKC activity. (B-E) DIV8 hippocampal neurons transfected with Caspr2 (B-D) or the Nav1.2-C-terminus Δ1871 fused with the CD4 reporter (NavCter) (E). Neurons were treated with Calphostin C (B,E), H89 (C), or DMSO (D), surface-labeled for HA (red), and stained for MAP2 (green). Soma of transfected neurons are indicated with asterisks and axons with white arrows. Control DMSO treatment had no effect on the polarized expression of Caspr2 (D). PKA inhibition by H89 did not modify the axonal targeting of the protein (C). Calphostin C (Calph) induced the nonpolarized expression of Caspr2 in the somatodendritic and axonal compartments (B), whereas it had no effect on the polarized expression of NavCter (E). (F,G) DIV8 hippocampal neurons transfected with Caspr2 were untreated (F) or treated with Calphostin C (G) and incubated for 1 hour at 37°C with Alexa-Fluor-594-conjugated transferrin (red) and anti-HA mAb to mediate internalization of Caspr2. Neurons were surface-labeled for HA (green) using Alexa Fluor 488 anti-rat immunoglobulins at 18°C. Cells were fixed, permeabilized and the internalized pool of HA-tagged Caspr2 was stained (blue). Calphostin C strongly inhibited the internalization of Caspr2 but had no effect on transferrin uptake. Scale bars: 15 μm (B-E) and 5 μm (F,G). (H) GST and the cytoplasmic region of Caspr2 fused with GST were subjected to in vitro PKC phosphorylation followed by SDS-PAGE. Coomassie blue staining (left) and ^{32}P-incorporation revealed by autoradiography (right) are shown.

transferrin receptor. Caspr2 is found in a complex with Kv1 channels at the juxtaparanodes of myelinated axons. We showed that the C-terminal PDZ-binding motif is not implicated in the axonal targeting of Caspr2 as is also reported for Kv1.2 (Gu et al., 2003). PDZ proteins are preferentially implicated in the clustering of ion channels and membrane proteins within distinct membrane subdomains (Sheng and Sala, 2001), but do not seem to have a role in their initial targeting to axons. Recent data indicate that the PDZ-binding motif of Caspr2 is dispensable for its clustering with Kv1 channels at juxtaparanodes (Horresh et al., 2008).

The expression of a number of membrane molecules such as the sodium channel Nav1.2, VAMP, CB1 cannabinoid receptor and nicotinic receptor, is restricted to axons in a way that is dependent on their somatodendritic endocytosis (Garrido et al., 2001; Sampo et al., 2003; Leterrier et al., 2006; Xu et al., 2006). Furthermore, the cell adhesion molecule L1/NgCAM, which is strongly polarized to axons, is internalized in the somatodendritic compartment towards recycling endosomes, and is mainly addressed to axons along the transcytotic pathway (Wisco et al., 2003; Yap et al., 2008). Interestingly, L1-CAM, similarly to Caspr2, contains a FERM-binding motif at a site that overlaps an endocytosis motif, which mediates interaction with the clathrin-adaptor AP2 (Kamiguchi and Lemmon, 1998; Dickson et al., 2002).

Caspr2 colocalizes with EEA1- and transferrin-positive vesicles in the somatodendritic compartment and is recognized by the endocytic pathway. However, the cytosolic determinant of Caspr2 that underlies the somatodendritic internalization does not encompass a canonical internalization signal such as the dileucine or tyrosine-based motifs recognized by the adaptor protein complex of clathrin-coated vesicles (Bonifacino and Traub, 2003). Endocytosis of Caspr2 occurs selectively in the somatodendritic compartment. One possibility is that the endocytic machinery displays dendrite-specific adaptors or that the signal for Caspr2 endocytosis is masked in axons via post-translational modification or protein-protein interaction. Caspr2 endocytosis is regulated during the maturation of hippocampal neurons and becomes robust in the somatodendritic compartment from DIV7. This indicates that the endocytic signal of Caspr2 is inactive at early stages and that

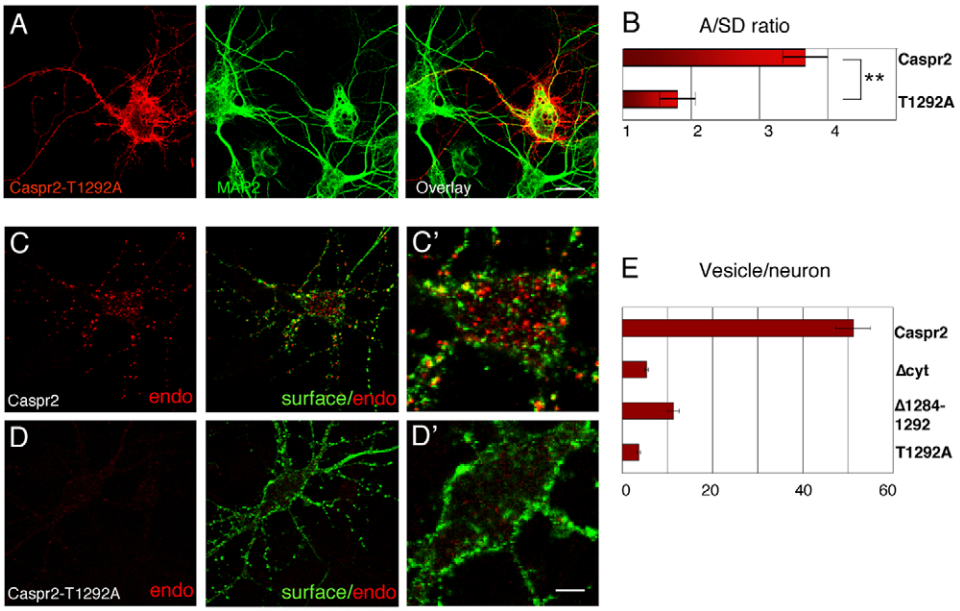

Fig. 6. The point mutation T1292A prevents the somatodendritic elimination of Caspr2. (A,C,D) DIV8 hippocampal neurons transfected with Caspr2-T1292A (A,D) or Caspr2 (C). (A) Neurons were surface-labeled for HA (red), and stained for MAP2 (green). (B) A/SD ratios. ANOVA indicates a significant difference between means (**P<0.01). (C,D) Neurons were incubated for 1 hour at 37°C with anti-HA mAb to mediate internalization of Caspr2. They were then surface-labeled for HA (green, surface), fixed, permeabilized, and the internalized pool of HA-tagged Caspr2 was stained (red, endo). C′ and D′ are enlarged images of the surface and internal overlays from C and D. (E) Quantification of the number of internalized vesicles per neuron for Caspr2, Caspr2Δcyt, Caspr2Δ1284-1292 and Caspr2T1292A. The point mutation T1292A prevented the somatodendritic elimination of Caspr2. Scale bars: 15 µm (A,C,D) and 6 µm (C′,D′).

it might be regulated by phosphorylation or through the binding of the FERM protein 4.1B. Unlike Caspr2, 4.1B distribution is nonpolarized in hippocampal neurons, but its activity might be locally or developmentally controlled. The binding of some FERM molecules to membrane proteins and the actin cytoskeleton has been shown to be negatively regulated by their ability to establish intramolecular associations. The open active conformation can be induced by phosphorylation or exposure to phosphoinositides (Tsukita et al., 1997; Girault et al., 1998). However, we showed that point mutations or a small deletion in the 4.1-binding motif of Caspr2, which should disrupt association with the scaffolding molecule, do not prevent the somatodendritic internalization or the axonal stabilization of mutated Caspr2.

We showed that the intracellular domain of Caspr2 can be phosphorylated by PKC in vitro and that the inhibition of PKC prevents the somatodendritic internalization of Caspr2 in hippocampal neurons. The point mutation T1292A within the endocytosis motif of Caspr2 also prevents removal of the mutated molecule from the somatodendritic surface, indicating that this residue is probably a phosphorylation substrate for PKC. One possibility is that the phosphothreonine within the Caspr2 endocytic motif is required for the binding of a clathrin adaptor. In addition, since this motif overlaps with the 4.1-binding site, phosphorylation at T1292 might disrupt association with the scaffolding molecule. Several channels, transporters and receptors are regulated by PKC for their surface stability and endocytosis (Martin and Henley, 2004; Herring et al., 2005; Holton et al., 2005). However, the mechanisms mediating the conditional trafficking signals are complex and are not completely elucidated. PKC-dependent phosphorylation of the GABA and glycine receptors might increase their dileucine-based endocytosis (Herring et al., 2005; Huang et al., 2007). PKC phosphorylation of the AMPA receptor subunit GluR2 at Ser880 stimulates its internalization through the disruption of interactions with the PDZ partners GRIP/ABP (Seidenman et al., 2003). We hypothesize that differential tuning of PKC kinase or phosphatase activity underlies the polarized and developmental regulated expression of Caspr2 at the cell membrane of hippocampal neurons.

The restricted distribution of membrane components along the axonal shaft at the nodes of Ranvier could be accomplished through different mechanisms. Such mechanisms might include sorting of membrane proteins into carriers along the secretory pathways and specific docking at the distinct axonal domains. In addition, membrane protein complexes can be trapped into each subdomain via adhesive contacts and scaffolding elements and eliminated elsewhere by endocytosis. In myelinated axons, Caspr2 is found in complex with Kv1 channels at the juxtaparanodes. However, it seems that neurons might adopt independent strategies for the axonal targeting of each element of the juxtaparanodal complex. Our data indicate that, in contrast to Kv1.2, Caspr2 does not contain a signal for its direct delivery to axons, and it travels within anterograde transport vesicles both in axons and dendrites. Thus, it appears unlikely that the constituents of the juxtaparanodal complex would be targeted to axons as a preformed complex, because distinct pathways are used for their axonal targeting. Caspr2 is implicated in the clustering of Kv1 channels at juxtaparanodes (Traka et al., 2003; Poliak et al., 2003). Protein kinases have direct and indirect effects on the membrane translocation and activity of the voltage-gated potassium channels (Yang et al., 2007; Connors et al., 2008). Our data indicate that PKC phosphorylation influences Caspr2 trafficking. The synergistic action of protein kinases on Caspr2 and Kv1 might have an important role in the fine-tuning of Kv1 channel function.

Materials and Methods

Cloning strategies

The pCDNA3-Caspr2 construct encoding human Caspr2 has been described previously (Bonnon et al., 2003). The HA epitope was inserted at the end of the signal peptide of Caspr2, between the residues W26 and T27. Site-directed mutagenesis was performed on Caspr2 cDNA in order to create a *Bam*HI restriction site between the nucleotides coding for these two amino acids. Complementary oligonucleotides encoding the HA epitope containing cohesive ends corresponding to the *Bam*HI restriction site were annealed and introduced in a pCDNA3-Caspr2 vector. Mutations and deletions were generated in the HA-tagged Caspr2 (Fig. 1). Caspr2Δcyt and Caspr2ΔCter were obtained using directed mutagenesis (Quikchange II mutagenesis kit, Stratagene) by insertion of a stop codon at residues 1285 and 1306, respectively. Caspr2Δ4.1, Caspr2Δ1284-1292 and Caspr2Δ1293-1305 were obtained by PCR amplification and insertion into the *Xba*I-*Bsp*EI sites of HA-tagged Caspr2. Caspr2-AGLI, Caspr2-EWAA, Caspr2-T1292A, Caspr2-Y1293F and Caspr2-H1294A were obtained using directed mutagenesis. Caspr2-GFP was generated by PCR amplification of the GFP inserted just after the signal peptide (residue 27) using directed mutagenesis. The GFP-Caspr2cyt chimera was generated by PCR amplification of the transmembrane and intracellular regions of Caspr2 (residues 1261-

1331) inserted into the *Xho*I-*Bam*HI sites of pEGFP-C1 (Clontech), modified with the insertion of the NrCAM signal peptide and HA epitope in *Nhe*I-*Age*I sites upstream of the GFP coding sequence (Falk et al., 2004). All constructs were verified by sequencing (CoGenics, Meylan, France). GFP-NrCAM-cyt includes the NrCAM signal peptide and HA epitope upstream and the NrCAM transmembrane and intracellular regions downstream of the GFP (Falk et al., 2004). The DNA constructs encoding GFP-tagged Dynamin-1 and Dynamin-1-K44A and the Nav1.2-C-terminus Δ1871 fused with the CD4 reporter have been described (Damke et al., 1994; Garrido et al., 2001). For expression in *E. coli* of the glutathione *S*-transferase (GST) fusion protein GST-Caspr2, the cDNA fragment corresponding to the intracellular of Caspr2 was amplified by PCR and cloned in pGEX vectors (Pharmacia Biotech).

Antibodies

The anti-Caspr2 antibody was generated by immunizing rabbits with the intracellular region (residues 1284-1331) fused to GST (Traka et al., 2003). Rat anti-HA monoclonal antibody (mAb) was purchased from Roche, mouse anti-MAP2 mAb and rabbit anti-EEA1 antibody from Sigma, and mouse anti-Ankyrin-G mAb from Santa Cruz Biotechnology. Rabbit polyclonal anti-MAP2 was a kind gift from Jean-François Leterrier, CNRS UMR 6187, Poitiers, France (Leterrier and Eyer, 1992). Secondary antibodies conjugated to Alexa Fluor 488, Alexa Fluor 568 and Alexa Fluor 647 were purchased from Invitrogen.

Hippocampal cell culture and immunofluorescence staining

Primary hippocampal cell cultures were prepared from embryonic day 18 Wistar rats. All animal experiments were carried out according to the animal care and experimentation committee rules approved by CNRS. Hippocampi were dissected and collected in Ca^{2+} and Mg^{2+}-free Hanks' balanced salt solution (Invitrogen). Cells were dissociated with trypsin (Invitrogen) and plated at a density of 13×10^4 cells/cm^2 on poly-L-lysine (Sigma)-coated coverslips. The hippocampal neurons were cultured in Neurobasal (Invitrogen) supplemented with 2% B-27 (Invitrogen), 1% penicillin-streptomycin (Invitrogen) and 0.3% glutamine (Invitrogen) in a humidified atmosphere containing 5% CO_2 at 37°C. Hippocampal neurons were transfected using Lipofectamine 2000 according to the manufacturer's protocol (Invitrogen).

H89, Calphostin C and Dynasore (Sigma) stock solutions were prepared in dimethyl sulfoxide (DMSO). H89 (1 μM), Calphostin C (0.5 μM) activated by light exposure for 15 minutes and Dynasore (80 μM) were added in the culture medium. Control experiments were performed using DMSO diluted at 1:1000. The hippocampal neurons were transfected at DIV6 and inhibitors were added 30 hours after transfection for a period of 18 hours.

Immunostaining was performed on transfected neurons at DIV8. For surface immunostaining of HA-tagged Caspr2, live cells were incubated with rat anti-HA mAb diluted (1:100) in the culture medium for 30 minutes, rinsed with culture medium, incubated with Alexa-Fluor-conjugated secondary antibody diluted in the culture medium and fixed with 4% paraformaldehyde in phosphate-buffered saline (PBS) for 10 minutes. For double-staining with rabbit anti-MAP2 (1:2000), cells were then permeabilized with 0.1% Triton X-100 for 10 minutes and then incubated with primary and secondary antibodies diluted in PBS containing 3% bovine serum albumin (BSA). For double staining of HA-tagged Caspr2 and EEA1, cells were fixed with 4% paraformaldehyde and permeabilized with 0.1% Triton X-100 before immunostaining with rat anti-HA mAb (1:100) and rabbit anti-EEA1 antibody (1:1000) and secondary antibodies. After washing in PBS, cells were mounted in Mowiol (Calbiochem).

Immunoendocytosis assay

COS-7 cells were cultured in DMEM medium supplemented with 10% fetal calf serum (FCS) (Invitrogen) and transiently transfected using jetPEI according to the manufacturer's protocol (Ozyme). The immunoendocytosis test was performed using rat anti-HA mAb (1:100) in culture medium for 1 hour at 4°C. After three washes with DMEM to eliminate unbound antibody, cells were either immediately fixed with 4% paraformaldehyde in PBS for 10 minutes or incubated in the culture medium for 30 minutes at 37°C and then fixed with paraformaldehyde. Cells were permeabilized and immunostained with anti-EEA1 antibody and secondary antibodies as described above.

Surface and internalized pools of Caspr2-HA were labeled in transfected neurons at DIV8. Live cells were incubated with rat anti-HA mAb diluted (1:100) in the culture medium for 1 hour at 37°C, then surface labeling was performed using Alexa-Fluor-488-conjugated secondary antibodies at 18°C to further block internalization. After fixation with 4% paraformaldehyde, cells were incubated with unconjugated secondary antibodies (0.2 mg/ml) for saturation, and then permeabilized before staining of the internalized pool using Alexa-Fluor-568-conjugated secondary antibodies. For endocytosis assays coupled with transferrin uptake, neurons were first incubated in the neurobasal medium without B27 for 1 hour, then incubated for 1 hour at 37°C with Alexa-Fluor-594-conjugated transferrin (0.1 mg/ml) and anti-HA mAb and labeling of the surface and internalized pools of Caspr2-HA was carried out as described above.

In vitro PKC phosphorylation assay

GST and GST-fusion proteins were expressed in *E. coli* and purified according to the recommendations of the manufacturer of pGEX vectors. In vitro kinase assays were carried out in a total volume of 20 μl containing 1.8 μM of GST-fusion protein (0.1 mg/ml), 25 mM Tris-HCl (pH 7.5), 10 mM $MgCl_2$, 0.1 mM EDTA, 2 μCi [γ-^{32}P]ATP, 100 μM ATP and 16 ng PKC (catalytic subunit from rat brain, Calbiochem), for 30 minutes at 30°C. The reaction was stopped by adding 5 μl of 5× Laemmli buffer. The phosphorylated proteins were separated by 12% SDS polyacrylamide gel electrophoresis and detected using the Image Reader FLA-7000 technology (Fujifilm). The GST-fusion proteins were visualized using Coomassie blue staining.

Confocal microscopy and image analysis

Confocal image acquisition was performed on a Leica TCS SP2 laser-scanning microscope equipped with 63× 1.32 NA oil-immersion objective. Images of GFP- or Alexa-Fluor-stained cells were obtained using the 488 nm band of an Argon laser and the 543 nm and 633 nm bands of an He-Ne laser for excitation. Spectral detection and emitted fluorescence were set as follows: 500-535 nm for Alexa Fluor 488 or GFP; 550-620 nm for Alexa Fluor 568 and Alexa Fluor 650; and 750 nm for Alexa Fluor 647. Fluorescence images were collected automatically as frame-by-frame sequential series, each image being produced from an average of three frame scans. The fluorescence of each image was resolved to obtain a minimum pixel fluorescence value of 255.

To determine the percentage of endocytic vesicles positive for Caspr2 constructs, confocal *Z*-stacks were collected and the image that showed the highest number of EEA1-positive vesicles was selected. The number of vesicles positive for EEA1 only or positive for both EEA1 and Caspr2 was determined with ImageJ software (NIH, http://rsb.info.nih.gov/ij/) in 20 neurons for each construct. The fluorescence ratio between axon and somatodendritic compartments (A/SD ratio) was determined after live immunostaining for HA with ImageJ. Two or three regions of interest were selected on confocal sections along the axonal and somatodendritic compartments, black pixels were eliminated (fluorescence=0), and the mean grey value was evaluated. The A/SD ratio was calculated in 20 neurons for each Caspr2 construct.

We wish to thank Marion Benoist, Bénédicte Dargent, Christophe Leterrier and Jérôme Devaux for helpful discussions, Marie-Pierre Blanchard and Christophe Leterrier for help with videomicroscopy. This work was supported by the Agence Nationale de la Recherche (C.F.-S. and L.G.), Association pour la Recherche sur la Sclérose en Plaques (fellowship to C.B.), and the National Multiple Sclerosis Society (C.F.-S. and L.G.).

References

Arnold, D. B. (2007). Polarized targeting of ion channlels in neurons. *Eur. J. Physiol.* **453**, 763-769.

Bonifacino, J. S. and Traub, L. M. (2003). Signals for sorting of transmembrane proteins to endosomes and lysosomes. *Annu. Rev. Biochem.* **72**, 395-447.

Bonnon, C., Goutebroze, L., Denisenko-Nehrbass, N., Girault, J. A. and Faivre-Sarrailh, C. (2003). The paranodal complex of F3/contactin and caspr/paranodin traffics to the cell surface via a non-conventional pathway. *J. Biol. Chem.* **278**, 48339-48347.

Brophy, P. J. (2001). Axoglial junctions: separate the channels or scramble the message. *Curr. Biol.* **11**, R555-R557.

Burbach, J. P. H. and Van der Zwaag, B. (2009). Contact in the genetics of autism and schizophrenia. *Trends Neurosci.* **32**, 69-72.

Connors, E. C., Ballif, B. A. and Morielli, A. D. (2008). Homeostatic regulation of Kv1.2 potassium channel trafficking by cyclic AMP. *J. Biol. Chem.* **283**, 3445-3453.

Damke, H., Baba, T., Warnock, D. E. and Schmid, S. L. (1994). Induction of mutant dynamin specifically blocks endocytic coated vesicle formation. *J. Cell Biol.* **127**, 915-934.

Denisenko-Nehrbass, N., Oguievetskaia, K., Goutebroze, L., Galvez, T., Yamakawa, H., Ohara, O., Carnaud, M. and Girault, J. A. (2003). Protein 4.1B associates with both Caspr/paranodin and Caspr2 at paranodes and juxtaparanodes of myelinated fibres. *Eur. J. Neurosci.* **17**, 411-416.

Dickson, T. C., Mintz, C. D., Benson, D. L. and Salton, S. R. (2002). Functional binding interaction identified between the axonal CAM L1 and members of the ERM family. *J. Cell Biol.* **157**, 1105-1112.

Eshed, Y., Feinberg, K., Poliak, S., Sabanay, H., Sarig-Nadir, O., Spiegel, I., Bermingham, Jr, J. R. and Peles, E. (2005). Gliomedin mediates Schwann cell-axon interaction and the molecular assembly of the nodes of Ranvier. *Neuron.* **47**, 215-229.

Fache, M. P., Moussif, A., Fernandes, F., Giraud, P., Garrido, J. J. and Dargent, B. (2004). Endocytotic elimination and domain-selective tethering constitute a potential mechanism of protein segregation at the axonal initial segment. *J. Cell Biol.* **166**, 571-578.

Falk, J., Thoumine, O., Dequidt, C., Choquet, D. and Faivre-Sarrailh, C. (2004). NrCAM coupling to the cytoskeleton depends on multiple protein domains and partitioning into lipid rafts. *Mol. Biol. Cell* **15**, 4695-4709.

Garrido, J. J., Fernandes, F., Giraud, P., Mouret, I., Pasqualini, E., Fache, M. P., Jullien, F. and Dargent, B. (2001). Identification of an axonal determinant in the C-terminus of the sodium channel Na(v)1.2. *EMBO J.* **20**, 5950-5961.

Garrido, J. J., Giraud, P., Carlier, F., Fernandes, F., Moussif, A., Fache, M. P., Debanne, D. and Dargent, B. (2003). A targeting motif involved in sodium channel clustering at the axonal initial segment. *Science* **300**, 2091-2094.

Girault, J. A. and Peles, E. (2002). Development of nodes of Ranvier. *Curr. Opin. Neurobiol.* **12**, 476-485.
Girault, J. A., Labesse, G., Mornon, J. P. and Callebaut, I. (1998). Janus kinases and focal adhesion kinases play in the 4.1 band: a superfamily of band 4.1 domains important for cell structure and signal transduction. *Mol. Med.* **4**, 751-769.
Gu, C., Jan, Y. N. and Jan, L. Y. (2003). A conserved domain in axonal targeting of Kv1 (Shaker) voltage-gated potassium channels. *Science* **301**, 646-649.
Gu, C., Zhou, W., Puthenveedu, M. A., Xu, M., Jan, Y. N. and Jan, L. Y. (2006). The microtubule plus-end tracking protein EB1 is required for Kv1 voltage-gated K+ channel axonal targeting. *Neuron* **52**, 803-816.
Herring, D., Huang, R., Singh, M., Dillon, G. H. and Leidenheimer, N. J. (2005). PKC modulation of GABAA receptor endocytosis and function is inhibited by mutation of a dileucine motif within the receptor beta 2 subunit. *Neuropharmacology* **48**, 181-194.
Heusser, K. and Schwappach, B. (2005). Trafficking of potassium channels. *Curr. Opin. Neurobiol.* **15**, 364-369.
Holton, K. L., Loder, M. K. and Melikian, H. E. (2005). Nonclassical, distinct endocytic signals dictate constitutive and PKC-regulated neurotransmitter transporter internalization. *Nat. Neurosci.* **8**, 881-888.
Horresh, I., Poliak, S., Grant, S., Bredt, D., Rasband, M. N. and Peles, E. (2008). Multiple molecular interactions determine the clustering of Caspr2 and Kv1 channels in myelinated axons. *J. Neurosci.* **28**, 14213-14222.
Horton, A. C. and Ehlers, M. D. (2003). Neuronal polarity and trafficking. *Neuron* **40**, 277-295.
Huang, R., He, S., Chen, Z., Dillon, G. H. and Leidenheimer, N. J. (2007). Mechanisms of homomeric alpha1 glycine receptor endocytosis. *Biochemistry* **46**, 12111-12123.
Kamiguchi, H. and Lemmon, V. (1998). A neuronal form of the cell adhesion molecule L1 contains a tyrosine-based signal required for sorting to the axonal growth cone. *J. Neurosci.* **18**, 3749-3756.
Lemaillet, G., Walker, B. and Lambert, S. (2003). Identification of a conserved ankyrin-binding motif in the family of sodium channel alpha subunits. *J. Biol. Chem.* **278**, 27333-27339.
Leterrier, C., Lainé, J., Darmon, M., Boudin, H., Rossier, J. and Lenkei, Z. (2006). Constitutive activation drives compartment-selective endocytosis and axonal targeting of type 1 cannabinoid receptors. *J. Neurosci.* **26**, 3141-3153.
Leterrier, J. F. and Eyer, J. (1992). Age-dependent changes in the ultrastructure and in the molecular composition of rat brain microtubules. *J. Neurochem.* **59**, 1126-1137.
Macia, E., Ehrlich, M., Massol, R., Boucrot, E., Brunner, C. and Kirchhausen, T. (2006). Dynasore, a cell-permeable inhibitor of dynamin. *Dev. Cell* **10**, 839-850.
Marfatia, S. M., Leu, R. A., Branton, D. and Chishti, A. H. (1995). Identification of the protein 4.1 binding interface on glycophorin C and p55, a homologue of the Drosophila discs-large tumor suppressor protein. *J. Biol. Chem.* **270**, 715-719.
Martin, S. and Henley, J. M. (2004). Activity-dependent endocytic sorting of kainate receptors to recycling or degradation pathways. *EMBO J.* **23**, 4749-4759.
Ogawa, Y., Horresh, I., Trimmer, J. S., Bredt, D. S., Peles, E. and Rasband, M. N. (2008). Postsynaptic density-93 clusters Kv1 channels at axon initial segments independently of Caspr2. *J. Neurosci.* **28**, 5731-5739.
Pearson, R. B. and Kemp, B. E. (1991). Consensus specificity motifs: tabulations. *Methods Enzymol.* **200**, 62-81.
Peles, E. and Salzer, J. L. (2000). Molecular domains of myelinated axons. *Curr. Opin. Neurobiol.* **10**, 558-565.
Poliak, S., Gollan, L., Martinez, R., Custer, A., Einheber, S., Salzer, J. L., Trimmer, J. S., Shrager, P. and Peles, E. (1999). Caspr2, a new member of the neurexin superfamily, is localized at the juxtaparanodes of myelinated axons and associates with K+ channels. *Neuron* **24**, 1037-1047.
Poliak, S., Salomon, D., Elhanany, H., Sabanay, H., Kiernan, B., Pevny, L., Stewart, C. L., Xu, X., Chiu, S. Y., Shrager, P. et al. (2003). Juxtaparanodal clustering of Shaker-like K+ channels in myelinated axons depends on Caspr2 and TAG-1. *J. Cell Biol.* **162**, 1149-1160.
Rasband, M. N., Park, E. M., Zhen, D., Arbuckle, M. I., Poliak, S., Peles, E., Grant, S. G. and Trimmer, J. S. (2002). Clustering of neuronal potassium channels is independent of their interaction with PSD-95. *J. Cell Biol.* **159**, 663-672.
Sampo, B., Kaech, S., Kunz, S. and Banker, G. (2003). Two distinct mechanisms target membrane proteins to the axonal surface. *Neuron* **37**, 611-624.
Schafer, D. P. and Rasband, M. N. (2006). Glial regulation of the axonal membrane at nodes of Ranvier. *Curr. Opin. Neurobiol.* **16**, 508-514.
Seidenman, K. J., Steinberg, J. P., Huganir, R. and Malinow, R. (2003). Glutamate receptor subunit 2 Serine 880 phosphorylation modulates synaptic transmission and mediates plasticity in CA1 pyramidal cells. *J. Neurosci.* **23**, 9220-9228.
Sheng, M. and Sala, C. (2001). PDZ domains and the organization of supramolecular complexes. *Annu. Rev. Neurosci.* **24**, 1-29.
Stephan, D. A. (2008). Unraveling autism. *Am. J. Hum. Genet.* **82**, 7-9.
Traka, M., Dupree, J. L., Popko, B. and Karagogeos, D. (2002). The neuronal adhesion protein TAG-1 is expressed by Schwann cells and oligodendrocytes and is localized to the juxtaparanodal region of myelinated fibers. *J. Neurosci.* **22**, 3016-3024.
Traka, M., Goutebroze, L., Denisenko, N., Bessa, M., Nifli, A., Havaki, S., Iwakura, Y., Fukamauchi, F., Watanabe, K., Soliven, B. et al. (2003). Association of TAG-1 with Caspr2 is essential for the molecular organization of juxtaparanodal regions of myelinated fibers. *J. Cell Biol.* **162**, 1161-1172.
Tsukita, S., Yonemura, S. and Tsukita, S. (1997). ERM proteins: head-to-tail regulation of actin-plasma membrane interaction. *Trends Biochem. Sci.* **22**, 53-58.
Ubersax, J. A. and Ferrell, Jr, J. E. (2007). Mechanisms of specificity in protein phosphorylation. *Nat. Rev. Mol. Cell Biol.* **8**, 530-541.
Waxman, S. G. and Ritchie, J. M. (1993). Molecular dissection of the myelinated axon. *Ann. Neurol.* **33**, 121-136.
Wisco, D., Anderson, E. D., Chang, M. C., Norden, C., Boiko, T., Fölsch, H. and Winckler, B. (2003). Uncovering multiple axonal targeting pathways in hippocampal neurons. *J. Cell Biol.* **162**, 1317-1328.
Xu, J., Zhu, Y. and Heinemann, S. F. (2006). Identification of sequence motifs that target neuronal nicotinic receptors to dendrites and axons. *J. Neurosci.* **26**, 9780-9793.
Yang, J. W., Vacher, H., Park, K. S., Clark, E. and Trimmer, T. S. (2007). Trafficking-dependent phosphorylation of Kv1.2 regulates voltage-gated potassium channel cell surface expression. *Proc. Natl. Acad. Sci. USA* **104**, 20055-20060.
Yap, C. C., Wisco, D., Kujala, P., Lasiecka, Z. M., Cannon, J. T., Chang, M. C., Hirling, H., Klumperman, J. and Winckler, B. (2008). The somatodendritic endosomal regulator NEEP21 facilitates axonal targeting of L1/NgCAM. *J. Cell Biol.* **180**, 827-842.

Journal of Cell Science